IN-24-CR
84775
P-29

WASHINGTON UNIVERSITY

DEPARTMENT OF PHYSICS

LABORATORY FOR ULTRASONICS

St. Louis, Missouri 63130

"Ultrasonic Nondestructive Characterization of Composites with 3-Dimensional Architectures"

Semiannual Progress Report: September 15, 1991 - March 14, 1992

NASA Grant Number: NSG-1601

Principal Investigator:

Dr. James G. Miller

Professor of Physics

The NASA Technical Officer for this grant is:

Dr. Joseph S. Heyman

NASA Langley Research Center

Hampton, Virginia

I. Introduction

The development and implementation of advanced composite material systems and their associated technologies are critical for success in the highly competitive world aerospace market. Acceptance of advanced production methods and field support of structures made with these new materials require the development of quantitative, cost-effective, inspection methods. In this Progress Report we present results of quantitative ultrasonic through-transmission imaging of composites with complex three-dimensional architecture using phase-insensitive and phase-sensitive techniques.

Ultrasonic inspection techniques which utilize more conventional piezoelectric transducers are sensitive to local variations in sign resulting from local variations in the phase of the incident pressure field across the face of the receiving transducer. Previous investigations have shown that these piezoelectric receivers can underestimate the total energy of an incident pressure field after propagation through inhomogeneous media or complex geometries.[1-11] Quantitative ultrasonic characterization of detrimental defects incurred during fabrication as well as in-service induced defects require an accurate estimate of total received energy. In this case a phase-insensitive measurement device may be a better choice as the receiving transducer. The phase-insensitive receiving devices and systems, which are insensitive to the local sign across the face of the receiving transducer, allow for the measurement of ultrasonic signals proportional to the power of the field. More accurate quantitative estimations of ultrasonic parameters related to inherent material properties, such as slope of attenuation (frequency dependence of signal loss), are achieved with measurement systems employing these power sensitive devices.

Inspection of composite structures over a stitched region joining substructures and/or the inspection of woven graphite/epoxy may represent situations where phase-cancellation effects can affect the ability to perform quantitative nondestructive evaluation measurements. In this Report we present the results of a quantitative interrogation of Kevlar™ stitched regions of a graphite/epoxy specimen using a phase-insensitive measurement technique. The results of narrowband, through-transmission, phase-insensitive (acoustoelectric), signal loss measurements of stitched and woven regions of a composite specimen are compared with conventional phase-sensitive scans of the same regions. The magnitude and variation of phase-sensitively and phase-insensitively measured frequency dependence of signal loss (quantified in the slope-of-attenuation parameter) are compared for the stitched region as well as a region of the composite not including the stitching.

II. Background

In a 1975 paper from our laboratory, Miller et al. explicitly described the process of phase cancellation across the face of a receiving transducer and the effects of this on echocardiographic measurements.[10] They proposed the use of a power-sensitive receiving transducer, based on the acoustoelectric effect, to reduce the phase-cancellation effects in ultrasonic measurements. In that same year (1975) Marcus and Carstensen reported large discrepancies between ultrasonic attenuation measurements of media obtained with a piezoelectric receiving transducer and measurements made with a radiation force balance.[9] Measurements made with the piezoelectric receiving transducers showed much more variation in the measured attenuation, especially in the case of highly inhomogeneous media.

Attenuation measurements, utilizing power-sensitive receiving transducers based on the acoustoelectric effect with CdS crystals, were implemented by Heyman et al.[2, 3] in advanced engineering materials and by Busse et al.[1] in tissue. Transmission attenuation measurements made with the phase-insensitive acoustoelectric receivers were shown to be free from phase-cancellation artifacts when compared to the same measurements obtained with phase-sensitive piezoelectric transducers. In addition, Busse et al. illustrated that phase-cancellation effects, inherent in phase-sensitive piezoelectric receivers, can be minimized by using small aperture transducers.[1] Refraction errors and phase-cancellation effects in ultrasonic computed tomography measurements were recognized by Klepper et al.[7, 8] and by Pan and Liu.[11] They recognized that measurements could overestimate the actual attenuation values of a material because of refraction of the ultrasonic beam.

III. Methods

Specimen

The specimen interrogated in this investigation was a section from a ballistically damaged composite panel obtained from McDonnell Aircraft Company. Figure 1 shows a schematic diagram of the panel. The original panel consisted of a series of unidirectional carbon/epoxy layers, configured in an unknown stacking sequence, with a total thickness of 0.19 cm. Two strips of woven carbon/epoxy lamina were laid down across the panel parallel to one another as indicated in the figure. Each strip was stitched to the surface of the panel with two rows of Kevlar™. The stitching runs from the woven surface straight through to the back surface of the panel where it is looped around and fed back through to the front surface. From this point the stitching runs along the front surface to the next through site. The exposed stitching on either side was pressed onto the surfaces so that each surface is flat. Each woven

strip was 5.4 cm in width and approximately 0.1 cm in depth. The woven strips were separated by 3.6 cm. In the region between the strips were two areas of damage imparted by ballistic impacts of projectiles. In order to accommodate our scanning apparatus the original panel was carefully cut into eight sections using a carbon blade saw. The specimen investigated for this study (see Figure 2) was a 15.7 cm by 9.5 cm section containing a woven strip and part of one of the ballistically damaged regions.

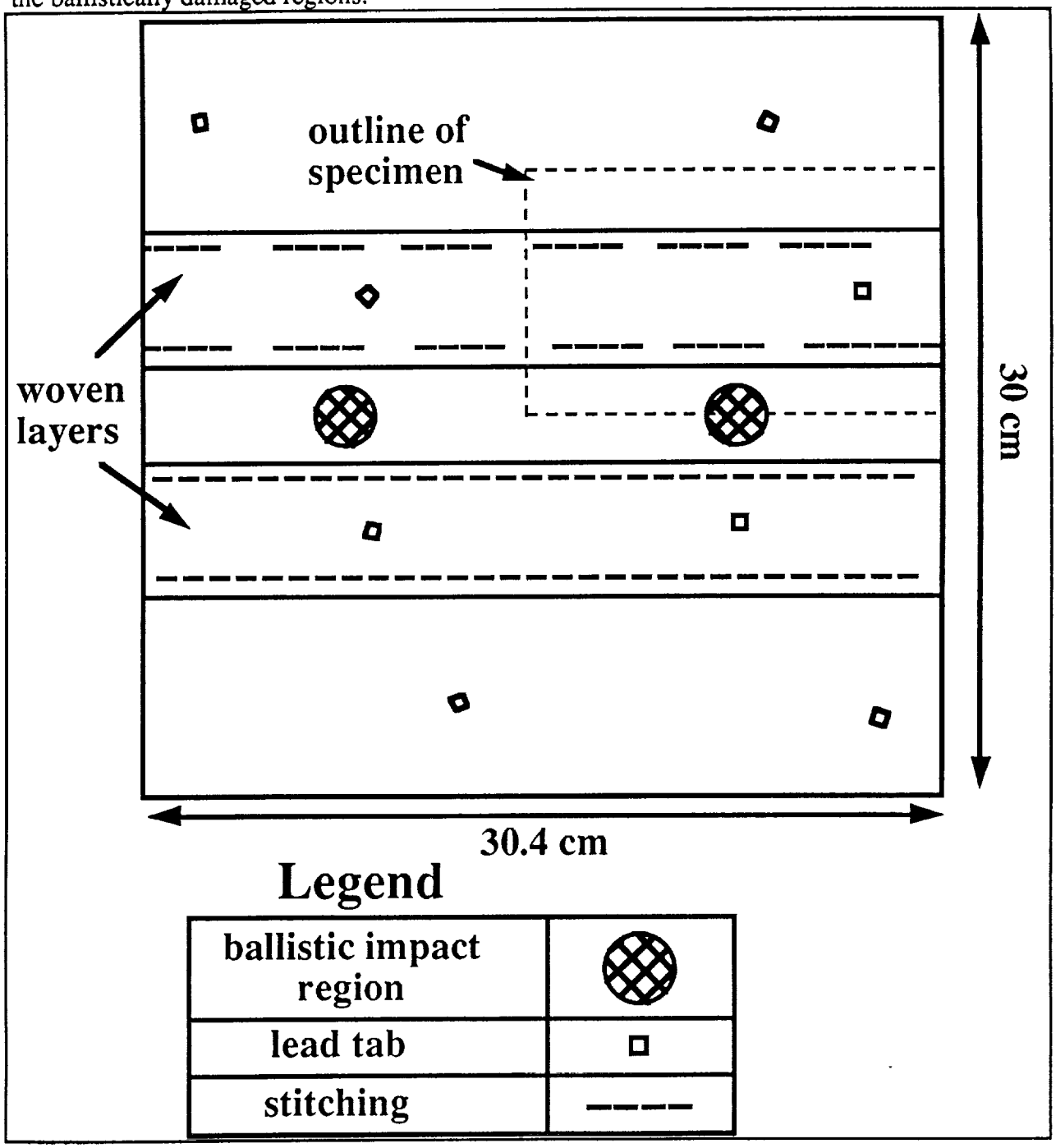

Figure 1. Schematic diagram of the ballistically damaged composite panel. The front (transmit side) view is shown.

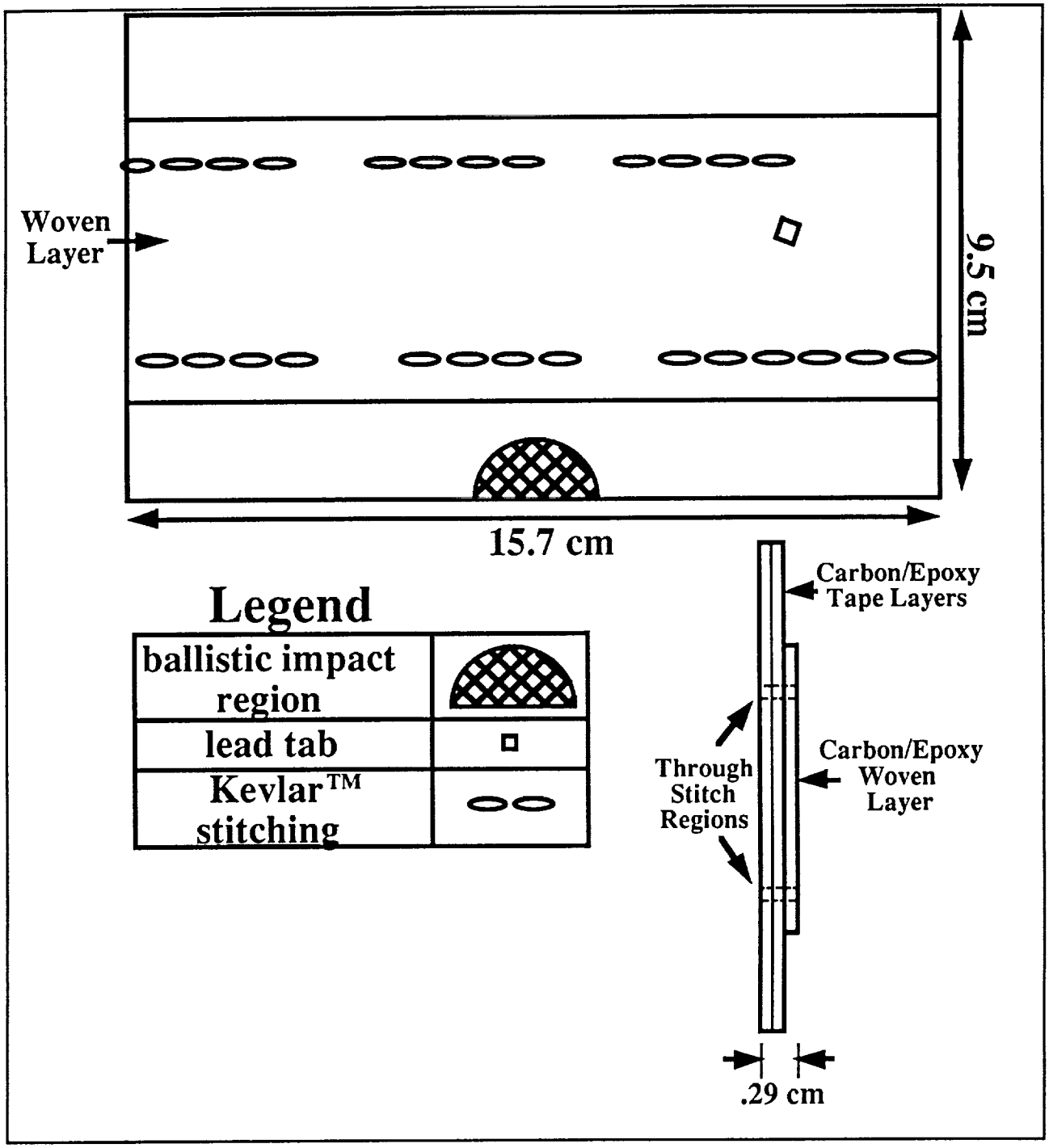

Figure 2. Schematic diagram of the specimen interrogated. The front and side views are shown. The specimen was scanned with the damaged end up; hence all subsequent grayscale images will have an upside-down orientation relative to the front view in this diagram.

Transducers

Both phase-sensitive and phase-insensitive through-transmission slope-of-attenuation measurements were performed in an immersion tank using the same 5 MHz center frequency, 0.5-inch diameter, broadband (Panametrics V309), focused (2-inch), piezoelectric transmitting transducer. For phase-sensitive measurements, a second 5 MHz, 0.5-inch diameter, 2.0-inch focal length, broadband, piezoelectric receiving transducer was employed. For the phase-insensitive measurements, a CdS acoustoelectric transducer was used as the receiving transducer. The CdS transducer utilizes the acoustoelectric effect to make phase-insensitive measurements. The presence of photo-induced charge carriers in the bulk CdS crystal is necessary for the acoustoelectric effect to occur. Hence, a 25-watt white light source was placed near the CdS transducer to ensure the proper conditions for its performance as a phase-insensitive receiver. In both types of measurements the ballistically damaged panel specimen was placed in the focal region of the transmitting transducer. For the phase-sensitive mode of interrogation, the piezoelectric receiving transducer was placed 2.0 inches from the specimen, a total of 4.0 inches from the transmitting transducer. In the phase-insensitive mode of interrogation, the CdS receiving transducer was placed approximately 2 mm from the back surface of the composite specimen to minimize the effects of refraction on the measurements.

Acquisition Systems

Figure 3a is a schematic block diagram showing the data acquisition system used in this investigation for the phase-sensitive measurements. The transmitted ultrasonic signal was a broadband pulse generated by a Metrotek MP215 pulser. As illustrated in the figure, the ultrasonic signal obtained from the receiving transducer was first sent through a pair of step attenuators (HP 355 series) which allow more precise adjustment of the signal amplitude to prevent saturation of the electronic equipment. The signal was then sent to a Metrotek MR101 receiving amplifier for further amplification before being sent to a Tektronix 2430A digital oscilloscope. The signal traces were then read by a Macintosh II computer and stored for further processing. At each position interrogated on the sample, 256 rf traces were captured from the scope, averaged, and analyzed as described below.

For the phase-insensitive mode of interrogation, illustrated in Figure 3b, a stepped, narrow-band approach was used. A HP3325A function generator was employed to produce a sine wave voltage output of a specified amplitude and frequency. This signal was fed into a coupled set of HP10534A mixer/modulators where it was gated with a 3 μsec gate. The resulting tone burst was amplified by an ENI broadband power amplifier before being sent to the

transmitting transducer. After propagation through the specimen, the through-transmitted ultrasonic signal was received by the CdS transducer. The CdS receiver output went directly into a Tektronix AM502 differential amplifier. In the differential amplifier the acoustoelectric signal was low-pass filtered to remove the piezoelectric response of the CdS receiver and amplified before being sent to the Tektronix 2430A digital oscilloscope where it was averaged 8 times. A Macintosh II computer took five readings of the peak voltage level of the averaged signals from the scope. The computer then calculated the average of the five read values and compared the new average value to a target value. If the signal level did not fall within a specified range near the target voltage, the drive level on the HP 3325A function generator was adjusted by the computer. The new output level of the received signal was once again compared with the target level. This process continued until the received signal output value fell within a previously specified range. Once this output condition was satisfied, the drive level on the HP 3325A function generator was recorded (in dBm) and the signal frequency incremented. Data were taken at eleven frequencies from 3 MHz to 7 MHz in 0.4 MHz steps for each point interrogated on the specimen.

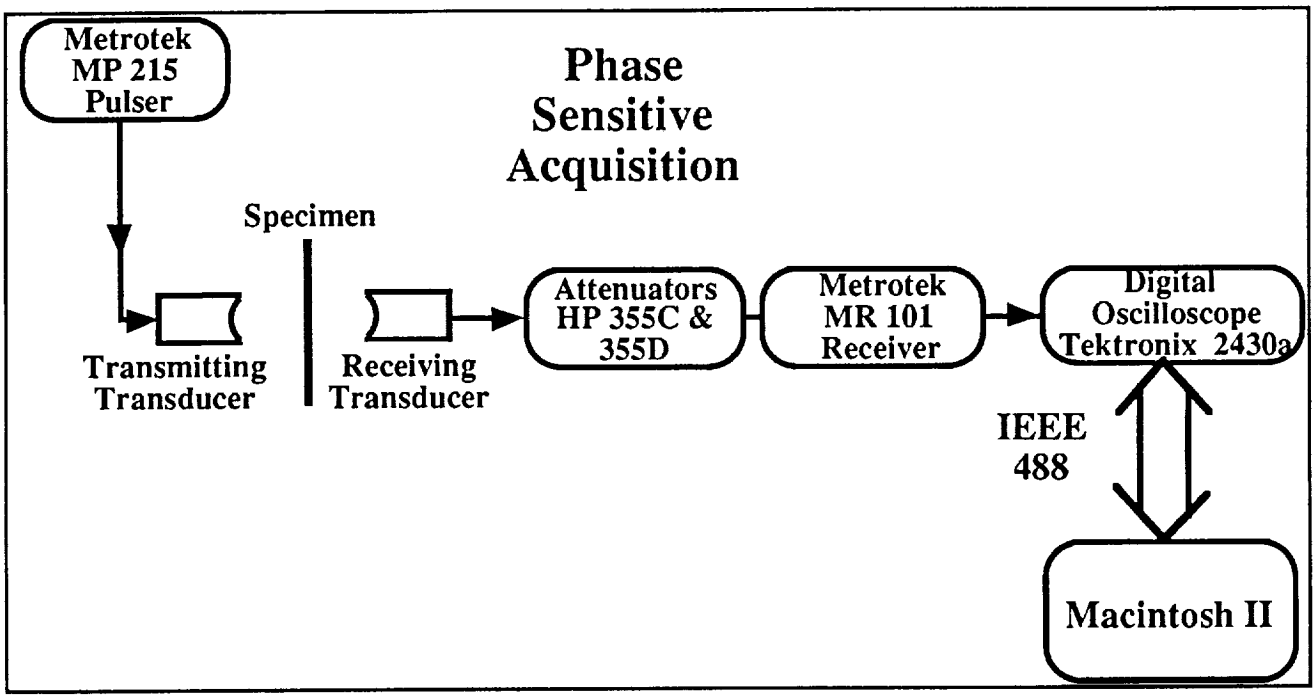

Figure 3a. Schematic block diagram showing phase-sensitive data acquisition system.

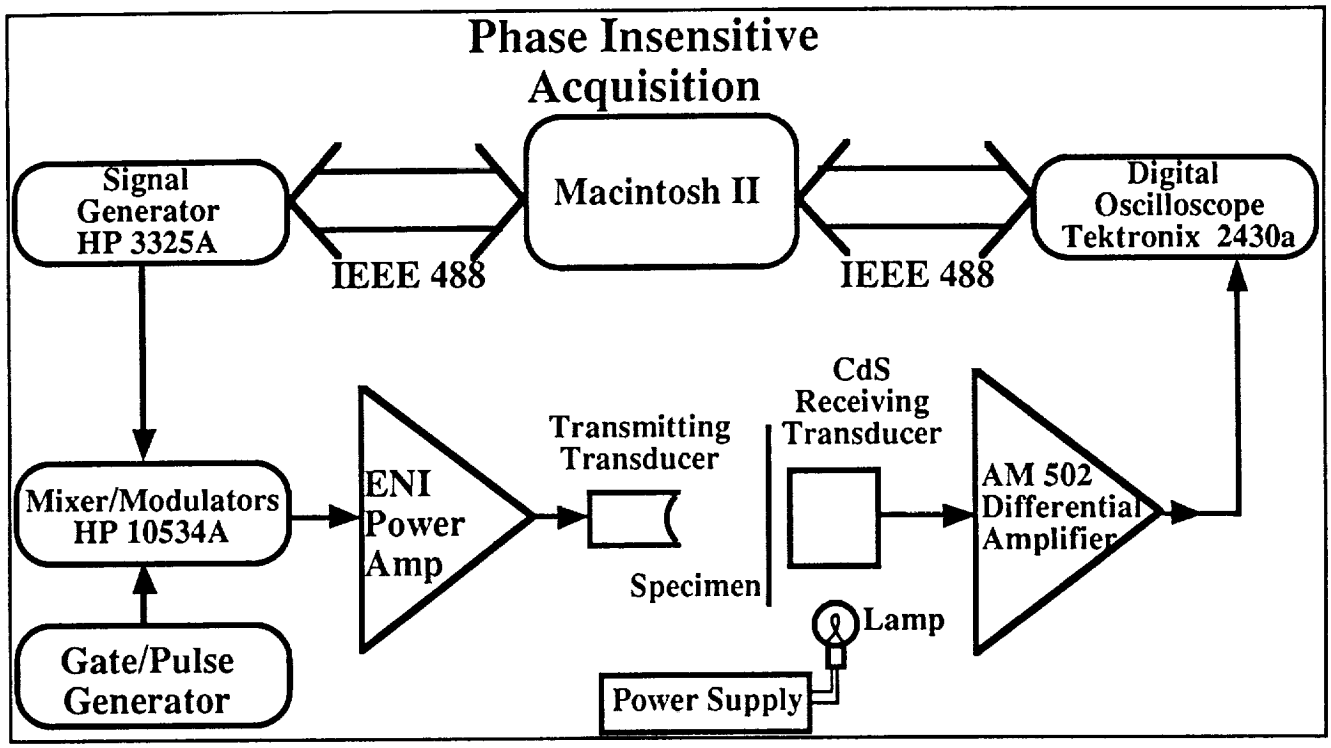

Figure 3b. Schematic block diagram showing phase-insensitive data acquisition system.

Phase-Sensitive and Phase-Insensitive Analyses

For the conventional phase-sensitive mode of interrogation, the digitized and signal-averaged through-transmitted rf waveform was processed for each site interrogated on the sample. As a first step, the mean value of the digitized rf signal was subtracted off in order to eliminate any dc offset that might exist in the recorded waveform. The power spectrum of the resultant zero-mean rf signal was then determined. The power spectrum of each data trace, expressed on a logarithmic scale, was subtracted from the power spectrum corresponding to a reference (water path only) trace also expressed on a logarithmic scale. The resultant signal loss data as a function of frequency were further characterized by performing a linear least-squares fit over the usable bandwidth (3 - 7 MHz) to determine the slope and intercept of the best straight line. The square of the correlation coefficient (R^2) was also determined in this process. The slope of the best fit line was normalized by the sample thickness to yield a value for slope-of-attenuation in dB/(cm-MHz).

For the phase-insensitive mode of interrogation, the drive levels recorded in dBm at each frequency were compared with the corresponding reference drive level values (water path only) required to give the same acoustoelectric response. The measured phase-insensitive acoustoelectric signal is proportional to the power of the received ultrasonic field. As long as the measurement system is linear, the output acoustoelectric voltage level read on the scope is

proportional to the input power. The linearity of our acoustoelectric system was previously verified over the dynamic range of our measurements. Thus, the difference between the reference drive level and the drive level required for each interrogated site yields the signal loss for each frequency. A straight line was fit to the phase-insensitive signal loss data in the same manner described above. Again, the resulting slope of the best fit line was normalized by the sample thickness to give slope-of-attenuation values for each site interrogated on the specimen.

IV. Results

A slope-of-attenuation image of the ballistically damaged specimen, obtained with the phase-sensitive measurement method described above, is illustrated in Figure 4a. Many distinct features of the sample can clearly be seen in this phase-sensitive image. The ballistically damaged region is readily identifiable in the top center portion of the image, and the two Kevlar™ stitch lines are readily apparent as are the borders of the woven layer. Because of the relatively long scan times involved, phase-insensitive (acoustoelectric) scans of the entire specimen were impractical. Thus, three distinct regions of the specimen were investigated phase-insensitively. Figure 4b delineates the three regions which were subsequently investigated acoustoelectrically for comparison with the phase-sensitive measurements. Region 1 runs along a stitched portion of the sample. This region seems to be relatively free of ballistic damage with the exception of a localized strip of visible surface damage. Region 2 is a portion along the other stitch line. This region encompasses part of the ballistically damaged area. Region 3 extends over a woven area, away from any stitched or damaged areas.

Figure 5a represents the acoustoelectric, phase-insensitive slope-of-attenuation image of Region 1. The grayscale levels in this image were optimized to best represent the acoustoelectric data. Figure 5b is the corresponding phase-sensitive slope image of the same region, displayed with the grayscale levels optimized for the range of slope values in this image. In order to quantitatively compare the phase-sensitive and phase-insensitive data, plots of the slope-of-attenuation values along lines in the respective images were made. Figure 6a illustrates the acoustoelectric slope data versus position along a line through the stitching. The specific line of values plotted is indicated by the arrow on Figure 5a. The slope data exhibit maxima where the stitching runs through the material. The phase-insensitive slope data range from 4.0 dB/(cm-MHz) to 10.0 dB/(cm-MHz) with an average value of 5.7 dB/(cm-MHz). (This excludes the last data point which is corrupted by edge effects.) An important component of the slope-of-attenuation analysis is the square of the correlation coefficient (R^2) for each slope value. In materials with complex structure such as stitched/woven composites, the degree of linearity of the signal loss with frequency over a specified bandwidth is important to consider in deciding how well the material can be characterized by slope-of-attenuation values. For this reason, it is necessary to include correlation information in making comparisons and drawing conclusions

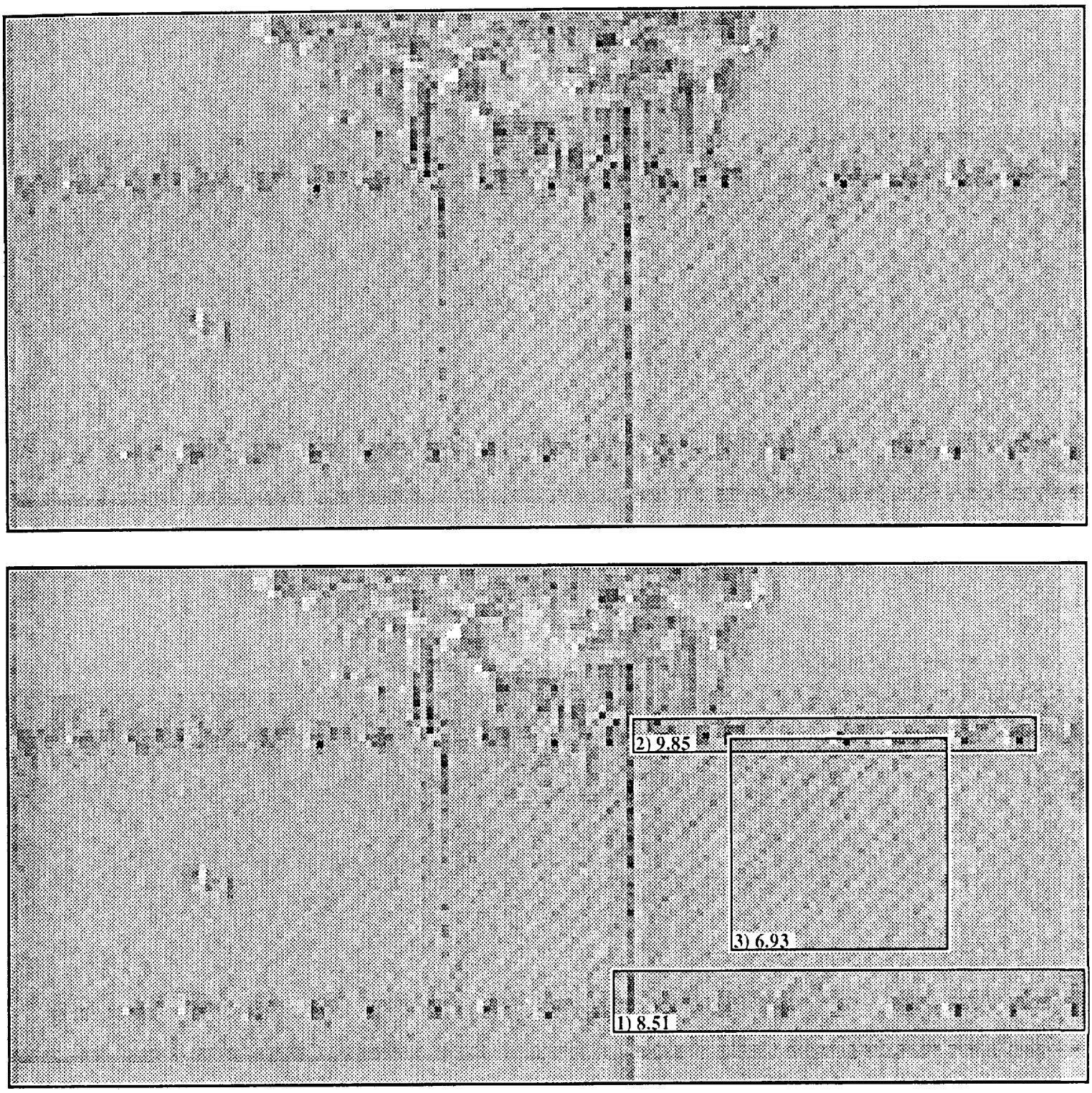

Figure 4 (a) Phase-sensitive slope-of-attenuation image of the entire specimen. The white pixels correspond to -7.5 dB/(cm-MHz) ; the black pixels correspond to 31.2 dB/(cm-MHz). Each pixel represents a 0.1 cm x 0.1 cm area on the sample.(b) Same image as shown in Figure 4a with the three regions of interest outlined.

from the slope data. Figure 6b is a plot of the square of the correlation coefficient of each point along the line. The R^2 values indicate that the signal loss has a highly significant linear relation to frequency for the number of points fit (N=11) over our measured bandwidth and thus confirm the validity of the slope-of-attenuation as a parameter for characterizing the material properties of this region. Figure 7a depicts a plot of the corresponding phase-sensitive slope data along the same stitch line. The line of data points illustrated in Figure 7a is indicated by the arrow on Figure 5b. These phase-sensitive values vary between 0.7 dB/(cm-MHz) and 23.8 dB/(cm-MHz) with an average of 10.8 dB/(cm-MHz). As Figure 7a illustrates, the phase-sensitive slope values vary over a much wider range than the corresponding acoustoelectric values. The phase-sensitive slope values also exhibit a wider variation in R^2 values than those obtained phase-insensitively. Even with the relatively large number of points fit (N=40) a few of the R^2 values indicate that phase-sensitive slope-of-attenuation characterization fails completely at certain points along the line. Furthermore, the phase-sensitive slope values are consistently larger than the corresponding phase-insensitive values, except for the data points where the R^2 value is small and our confidence in the slope value is minimal. The range and absolute value differences between the two data sets are illustrated in Figure 8 where both the phase-sensitive and phase-insensitive slope-of-attenuation values are plotted on the same graph.

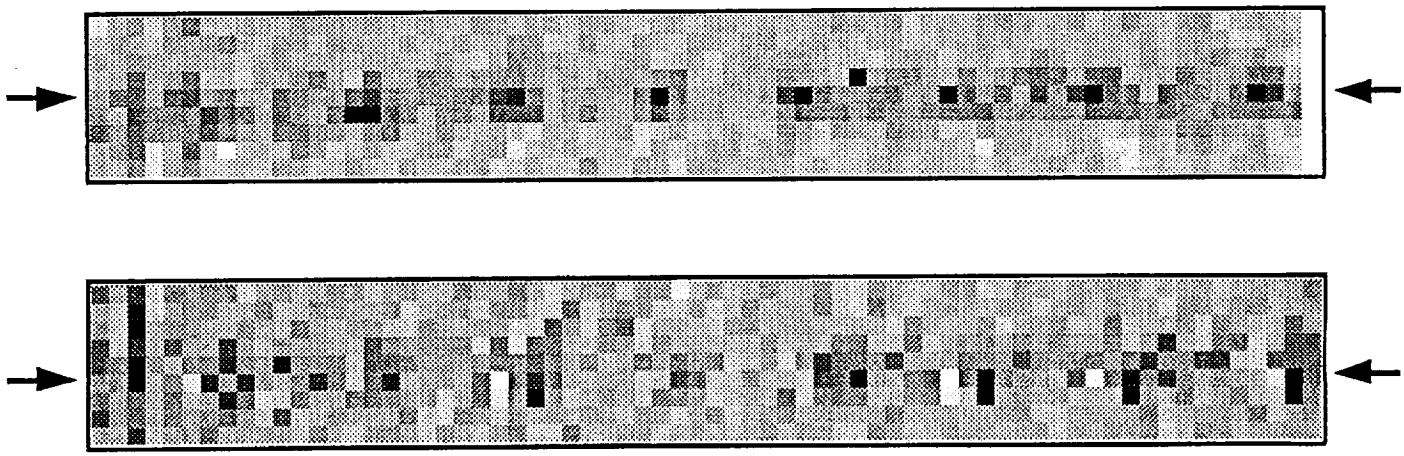

Figure 5. (a) Phase-insensitive, acoustoelectric slope-of-attenuation image of Region 1. The white pixels correspond to 2.1 dB/(cm-MHz) ; the black pixels correspond to 8.2. dB/(cm-MHz). (b) Phase-sensitive slope-of-attenuation image of Region 1. The white pixels correspond to 2.1 dB/(cm-MHz) ; the black pixels correspond to 20.5 dB/(cm-MHz).

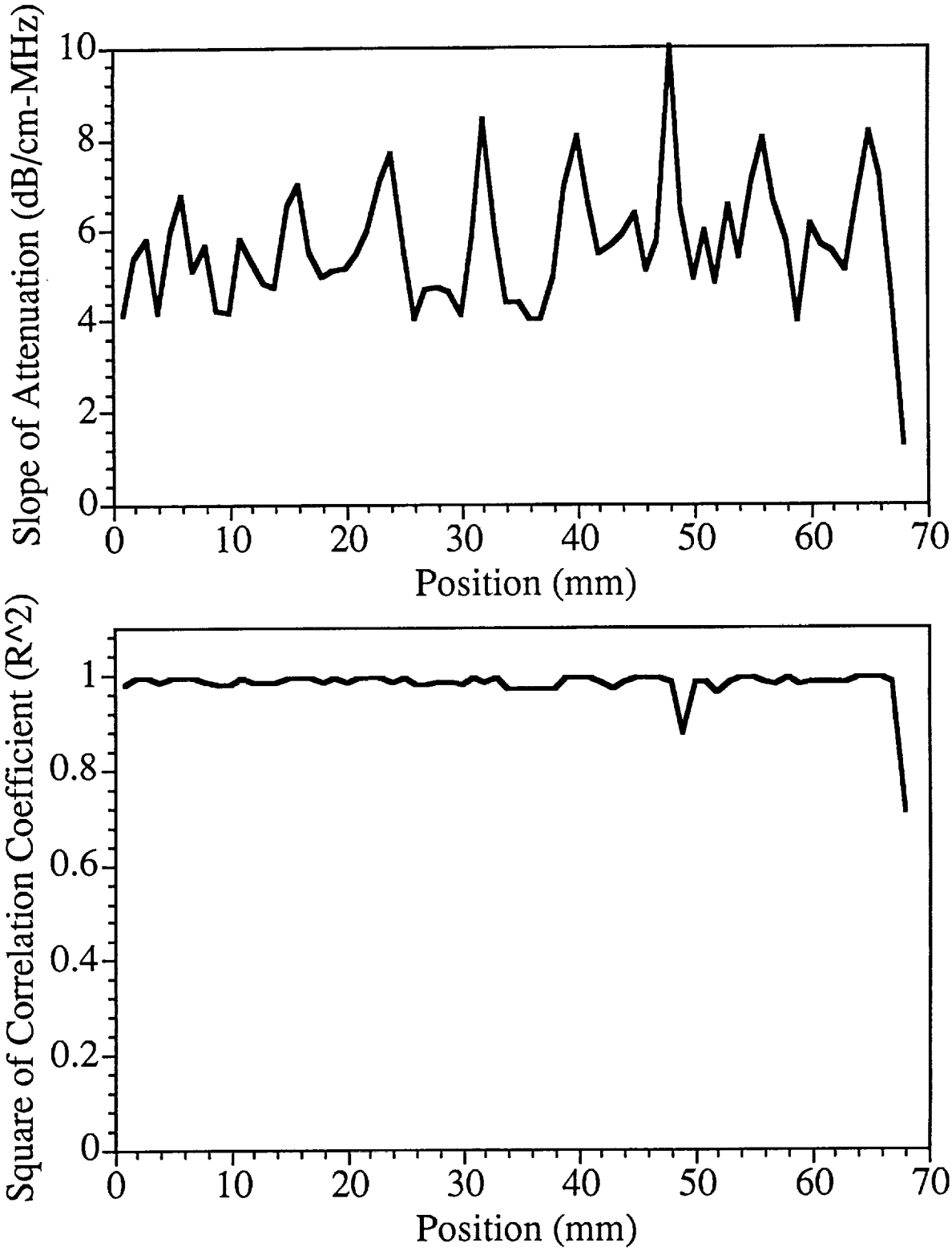

Figure 6 (a) Phase-insensitive slope-of-attenuation values over the stitch line in Region 1. (b) R^2 values for linear fit of phase-insensitive signal loss at each site along stitch line.

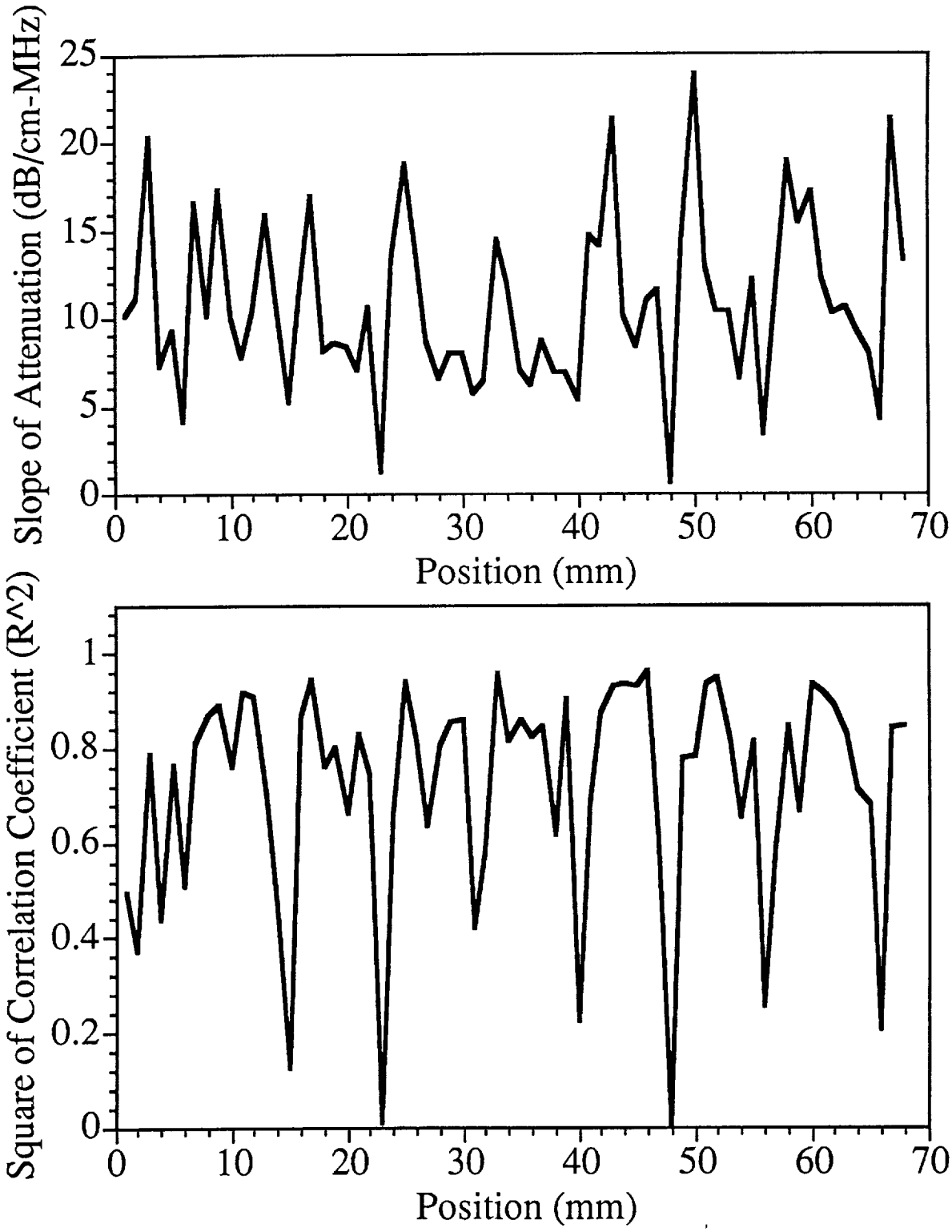

Figure 7 (a) Phase-sensitive slope-of-attenuation values over the stitch line in Region 1. (b) R^2 values for linear fit of phase-sensitive signal loss at each site along stitch line.

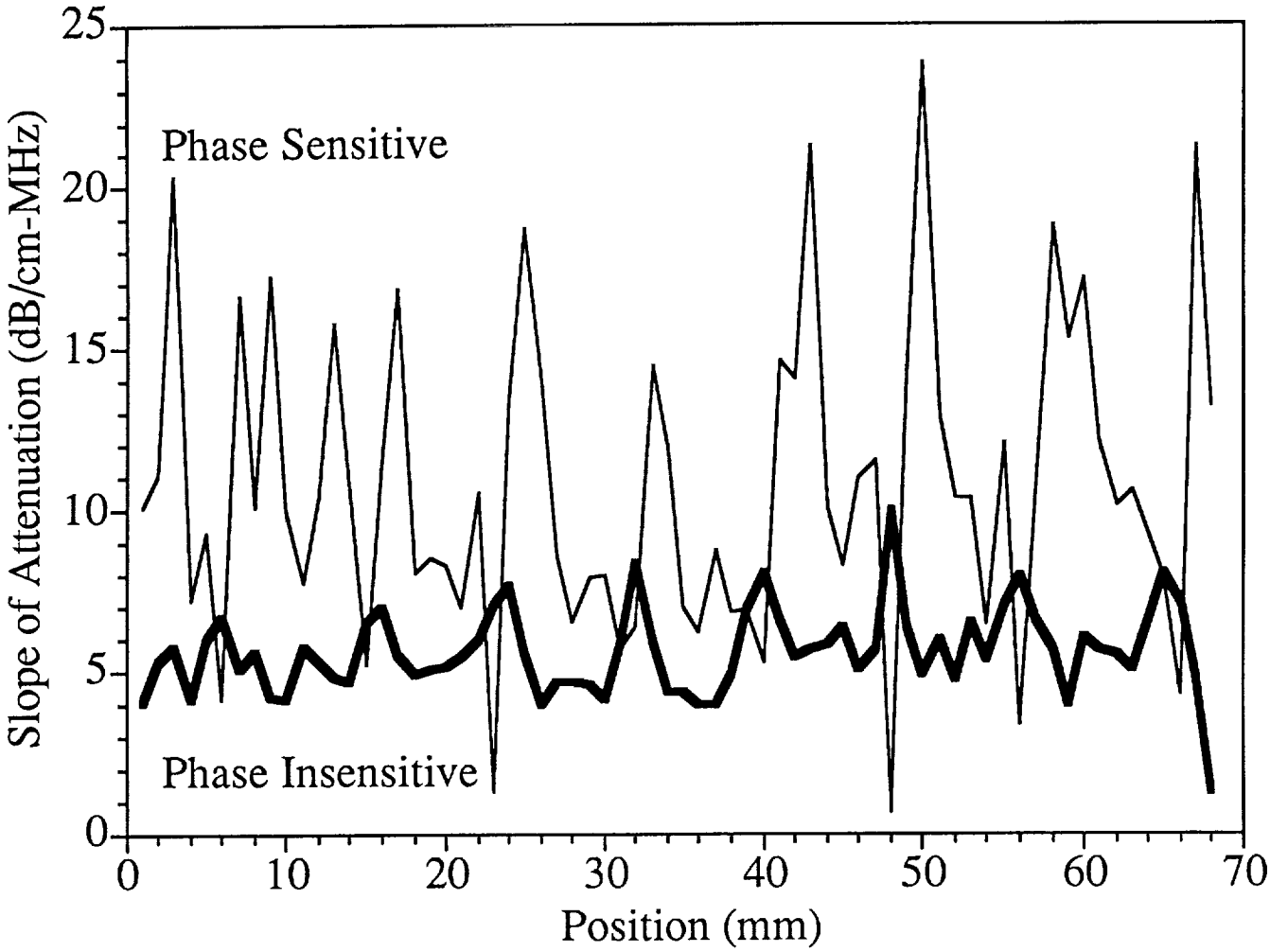

Figure 8. Phase-sensitive and phase-insensitive slope-of-attenuation values over the stitch line in Region 1.

A similar comparison of the phase-insensitive and phase-sensitive data from Region 2 was carried out. Figures 9a and 9b depict the acoustoelectric and phase-sensitive slope-of-attenuation images over the region, respectively. Again, the gray-level mapping of each image was optimized for its own respective data. Figures 10a and 10b are plots of the slope values and their associated R^2 values for the acoustoelectric data along a line through the stitching (indicated by the arrow in Figure 9a). Figures 11a and 11b are plots of the slope values and their associated R^2 values for the phase-sensitive data along the same line as through the stitching (indicated by the arrow in Figure 9b). Again, we observe that the phase-insensitive slope values all have associated R^2 values well above 0.9 (with the exception of two isolated points) whereas the phase-sensitive R^2 values vary widely. Also, the phase-sensitive slope values vary over a much larger range than the corresponding acoustoelectric data and the phase-sensitive values are typically larger in absolute value than the corresponding acoustoelectric values. Figure 12

displays both sets of data plotted on the same graph. Because Region 2 encompasses a damaged area, additional comparisons between the data sets were carried out. In both data sets, there appeared to be two distinct segments along the line. The two different domains can best be observed by comparing the local minimum values along each line. The two distinct segments may be characterized by taking the average of the slope values over the two respective domains. In both the phase-sensitive and phase-insensitive cases, a shift in the average value between the two portions of the line was observed. Figures 13a and 13b display the line plots and the segmented averages along the line for both data sets. The mean slope shift is of the same order in both cases. However, in the phase-sensitive case, the standard deviations of the slope values along the line are an order of magnitude larger than the level shift, whereas, in the acoustoelectric case, the standard deviation and the level shift are of the same order. The comparison of these parameters is illustrated in Figure 14.

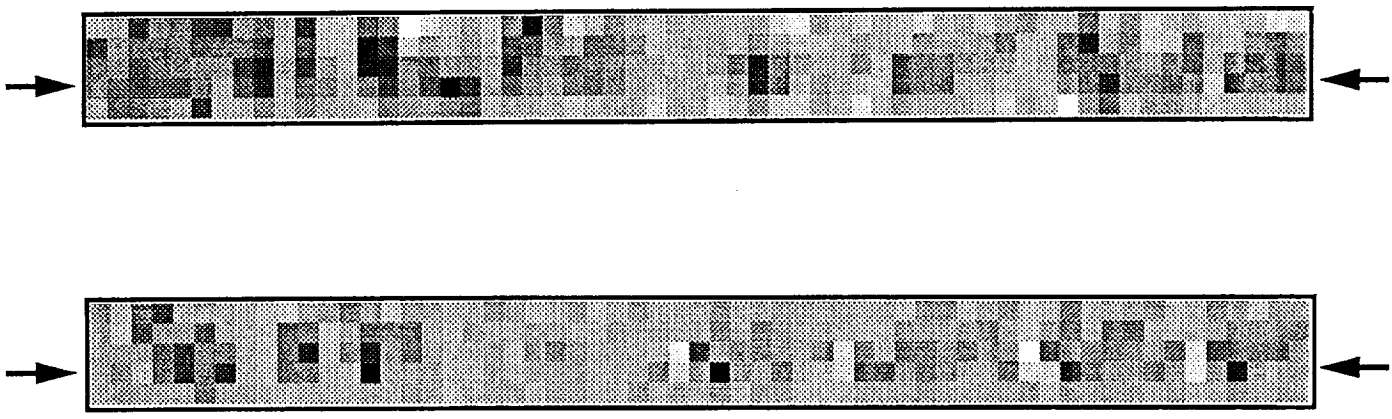

Figure 9 (a) Phase-insensitive, acoustoelectric slope-of-attenuation image of Region 2. The white pixels correspond to 2.7 dB/(cm-MHz) ; the black pixels correspond to 8.1 dB/(cm-MHz). (b) Phase-sensitive slope-of-attenuation image of Region 2. The white pixels correspond to -2.5 dB/(cm-MHz) ; the black pixels correspond to 28.9 dB/(cm-MHz).

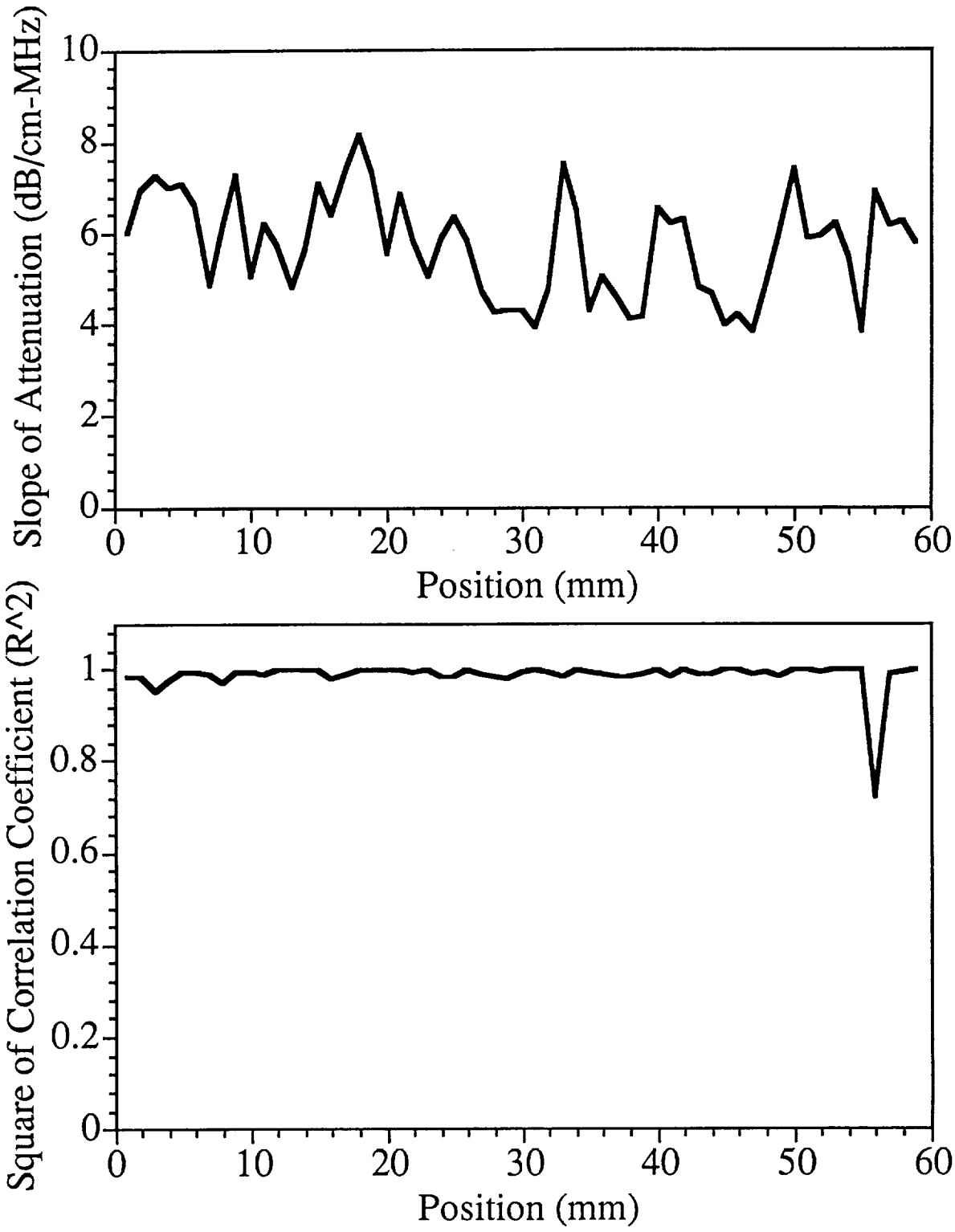

Figure 10 (a) Phase-insensitive slope-of-attenuation values over the stitch line in Region 2. (b) R^2 values for linear fit of phase-insensitive signal loss at each site along stitch line.

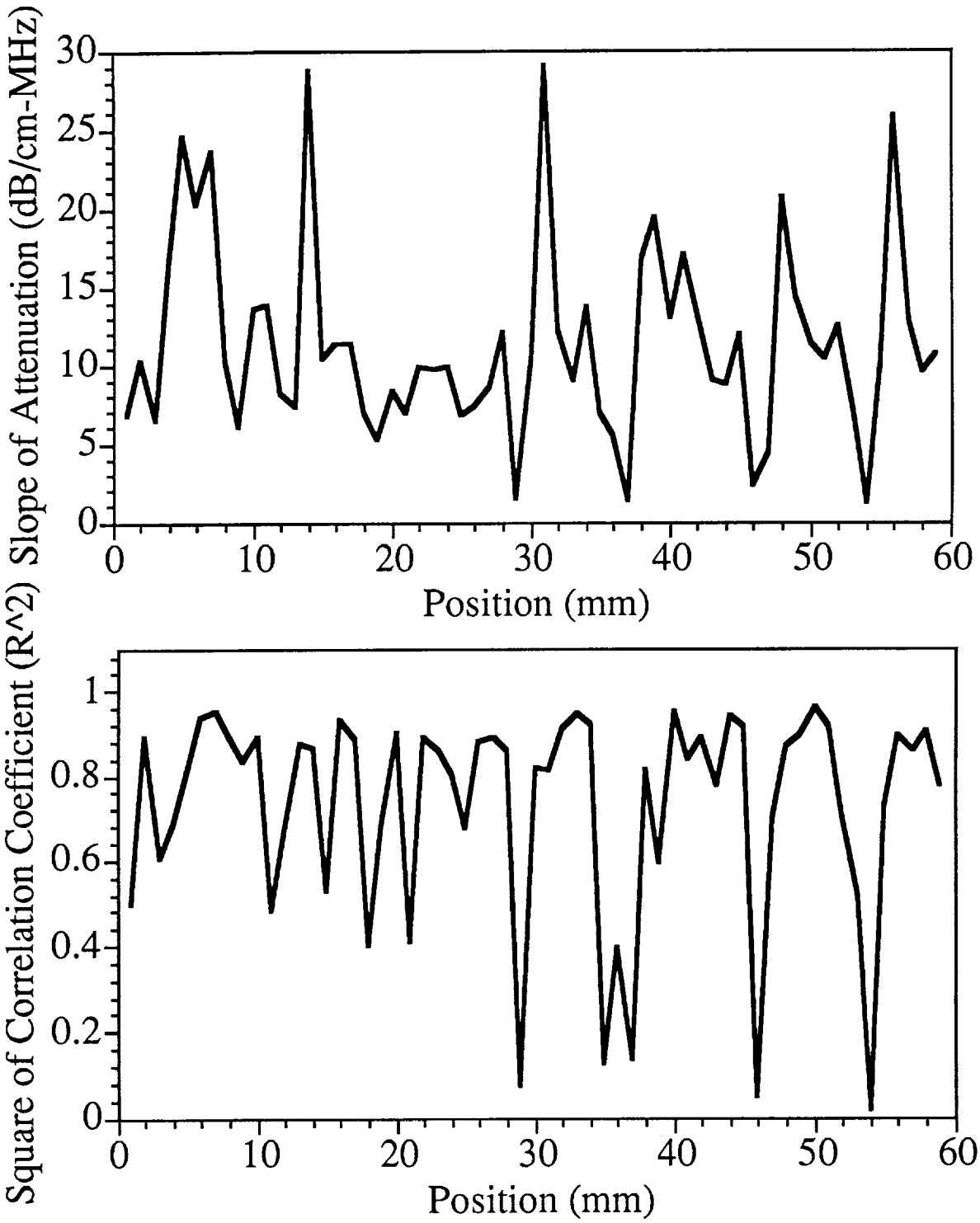

Figure 11 (a) Phase-sensitive slope-of-attenuation values over the stitch line in Region 2. (b) R^2 values for linear fit of phase-insensitive signal loss at each site along stitch line.

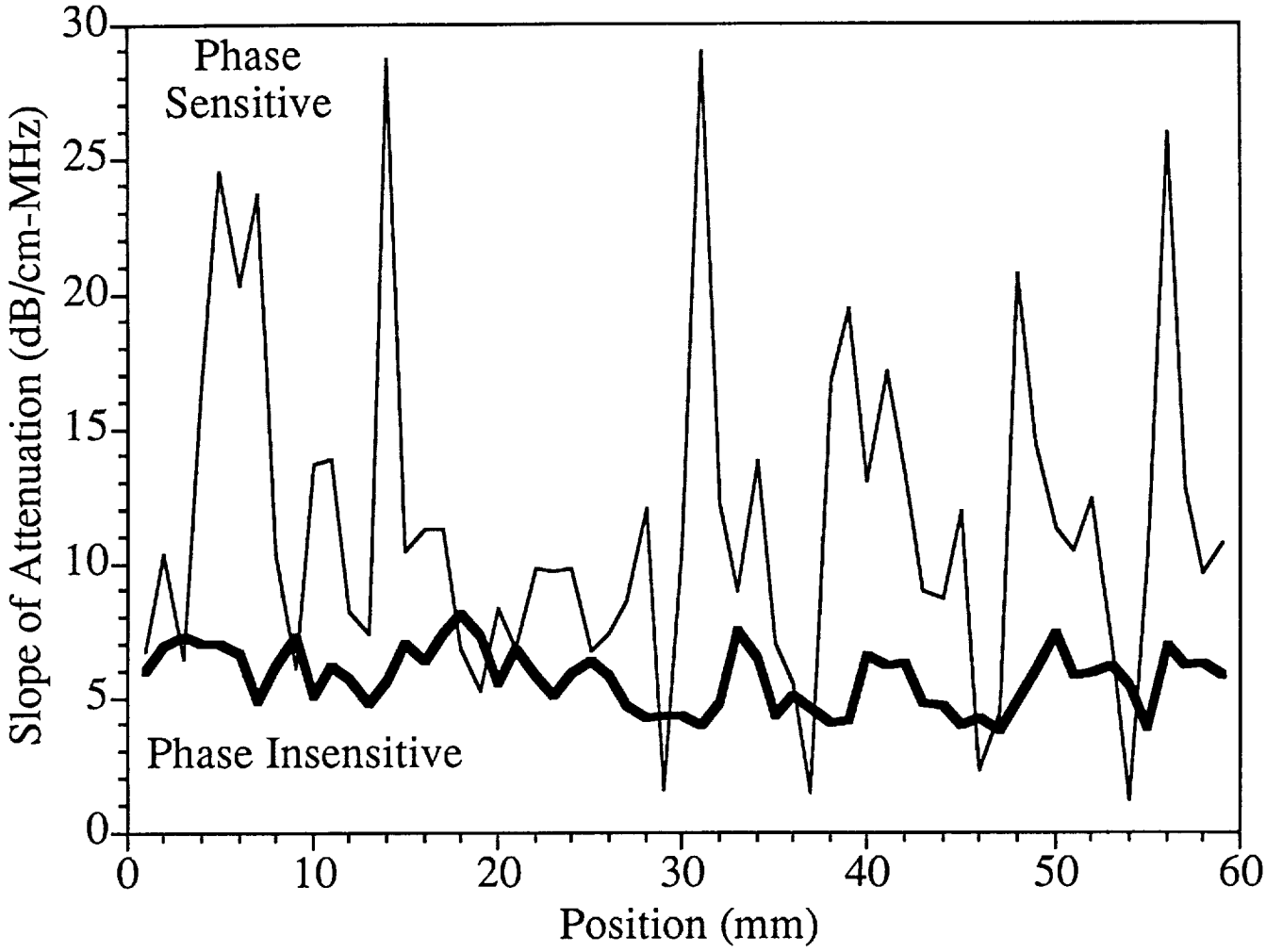

Figure 12. Comparison of the phase-insensitive, acoustoelectric and the phase-sensitive slope-of-attenuation values along the stitch line in Region 2.

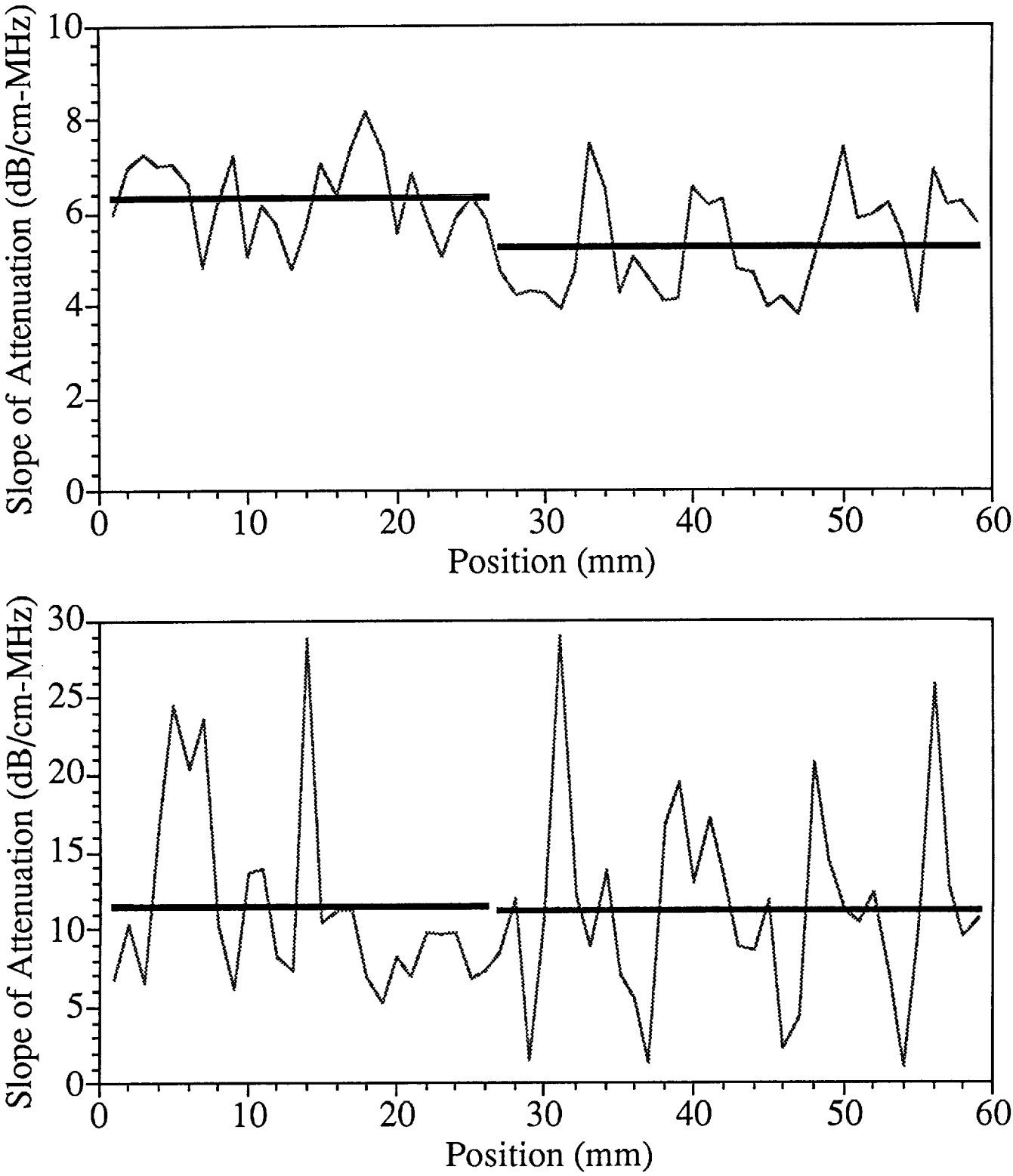

Figure 13 (a) Slope-of-attenuation plot for the acoustoelectric data over the stitch line in Region 2. (b) Slope-of-attenuation plot for the phase-sensitive data over the same stitch line. The average slope value for the damaged and undamaged regions is shown in both.

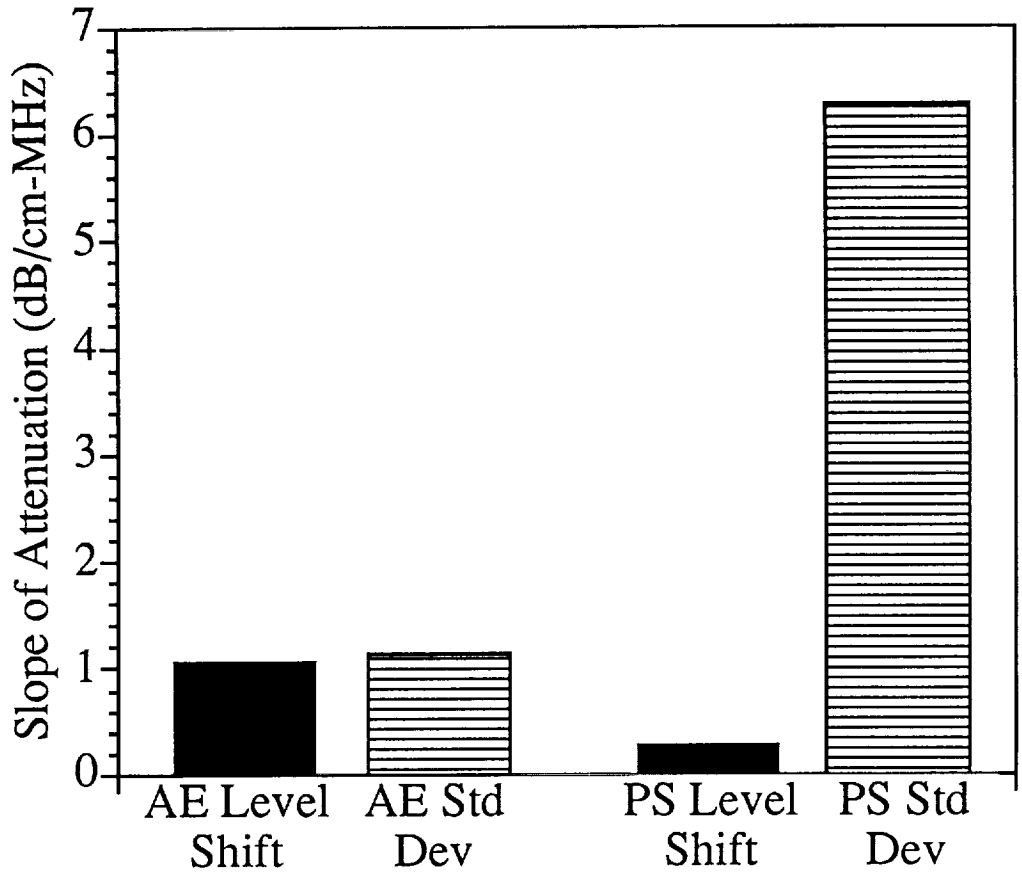

Figure 14. Column plot displaying the difference in the average value (level shift) between the two regions along the damaged stitch line and the standard deviation of the slope values along the line for both the acoustoelectric (AE) and phase sensitive (PS) data.

Figures 15a and 15b represent the respective acoustoelectric and phase-sensitive slope-of-attenuation images for Region 3. Again, these grayscale images were optimized over their own respective range of values. Figures 16a and 16b depict the slope-of-attenuation values and corresponding R^2 values for the acoustoelectric data obtained along the line shown by the arrow on Figure 15a. Figures 17a and 17b and 18a and 18b depict the slope and R^2 plots for the corresponding phase-sensitive data for the two lines marked by arrows on Figure 15b. Figures 19a and 19b illustrate the acoustoelectric and phase-sensitive values on the same graphs. As observed previously, the acoustoelectric slope values are lower in magnitude and vary over a smaller range than the corresponding phase-sensitive values. It may also be useful to consider the average properties of the material over an area large compared to the characteristic size of the weave pattern. Figure 20 displays the distribution of slope-of-attenuation values over Region 3 for both the acoustoelectric and phase-sensitive data. The average phase-insensitive slope-of-attenuation value over the region is 2.8 dB/(cm-MHz) with a standard deviation of 0.4 dB/(cm-

MHz). The phase sensitive measurements yielded an average of 7.0 (dB/cm-MHz) with a standard deviation of 1.7 (dB/cm-MHz).

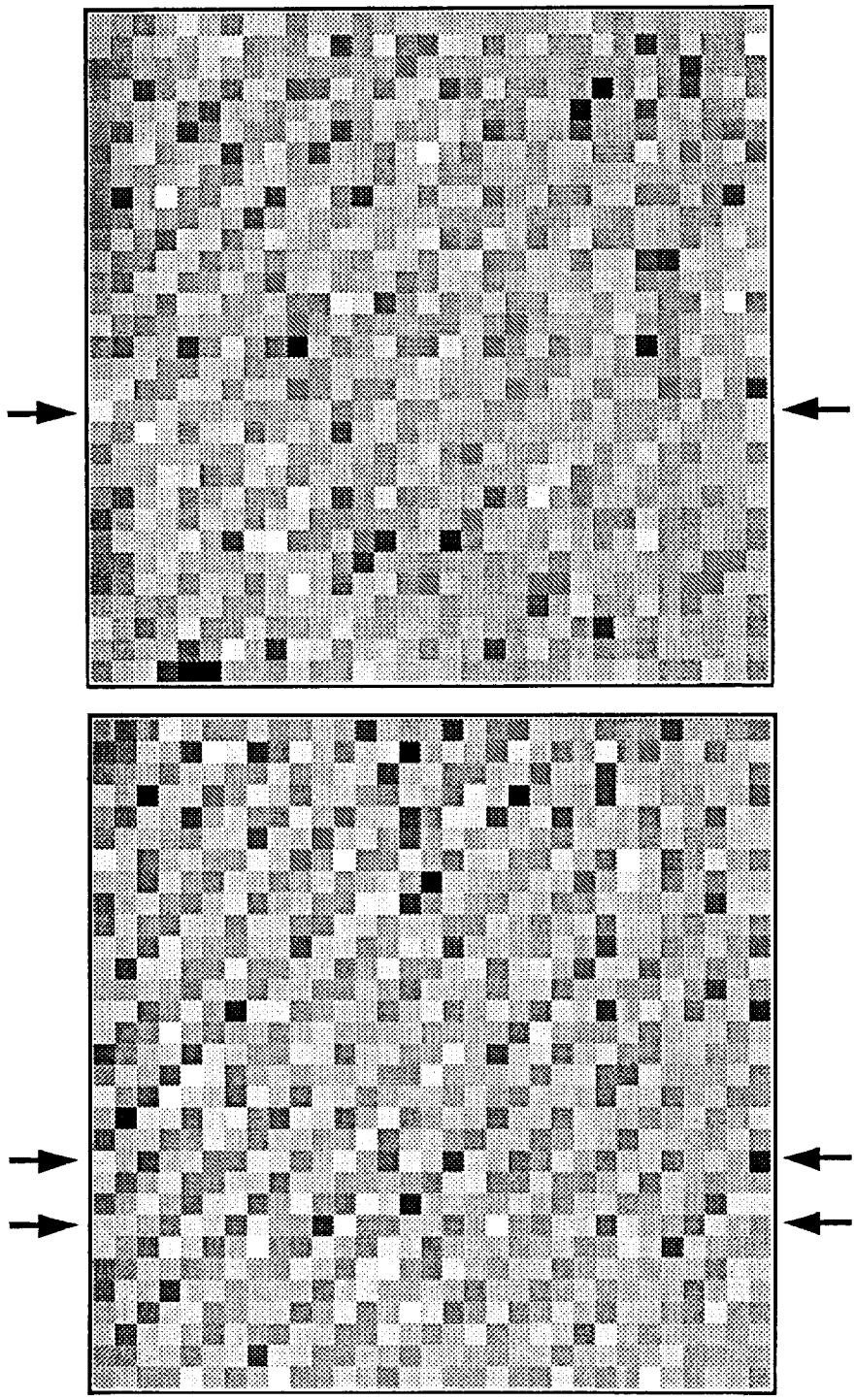

Figure 15 **(a)** Phase-insensitive, acoustoelectric slope-of-attenuation image of Region 3. The white pixels correspond to 1.9 dB/(cm-MHz) ; the black pixels correspond to 3.8 dB/(cm-MHz). **(b)** Phase-sensitive slope-of-attenuation image of Region 3. The white pixels correspond to 3.3 dB/(cm-MHz) ; the black pixels correspond to 12.1 dB/(cm-MHz).

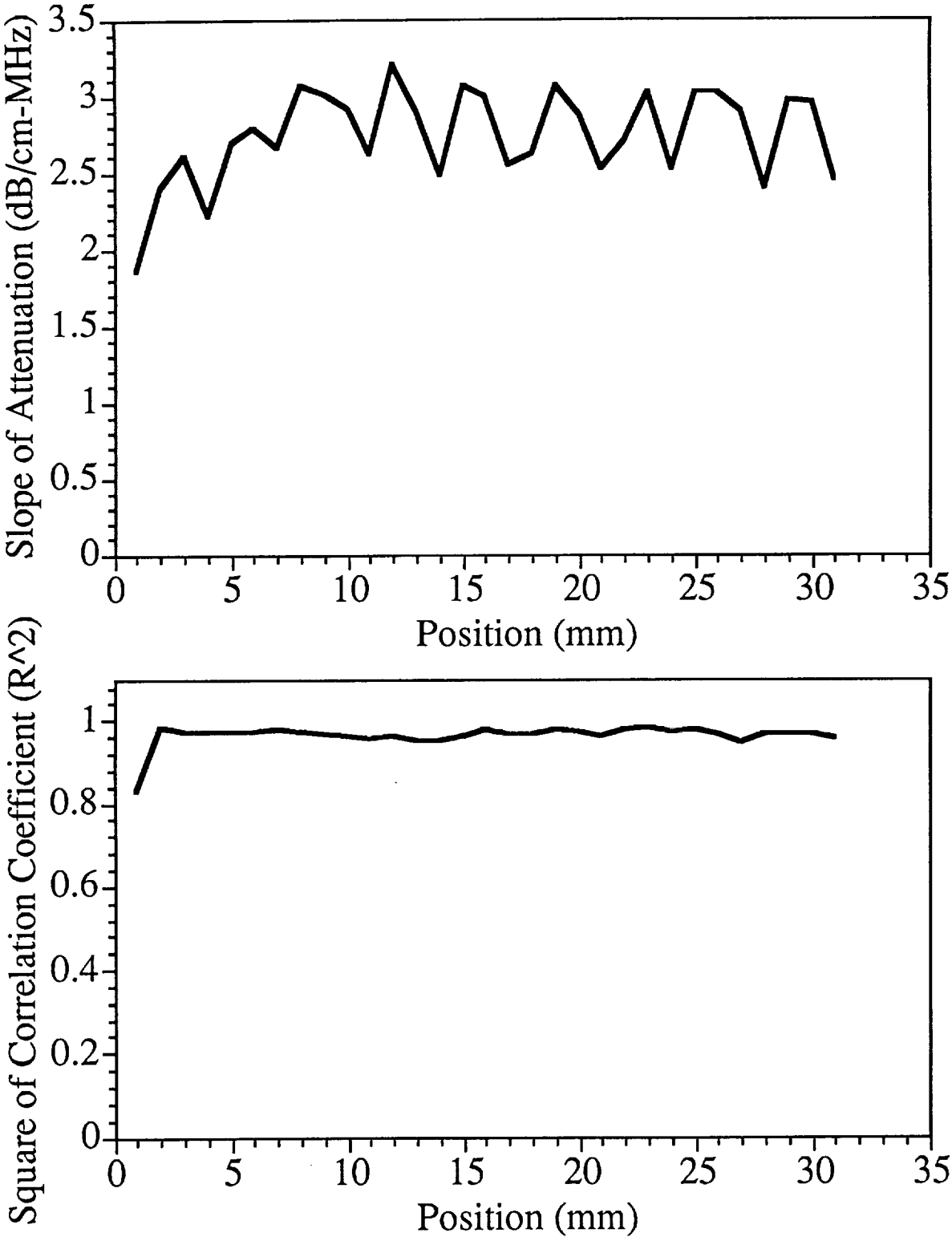

Figure 16 (a) Phase-insensitive slope-of-attenuation values over a line through Region 3. (b) R^2 values for linear fit of phase-insensitive signal loss at each site in Figure 16a.

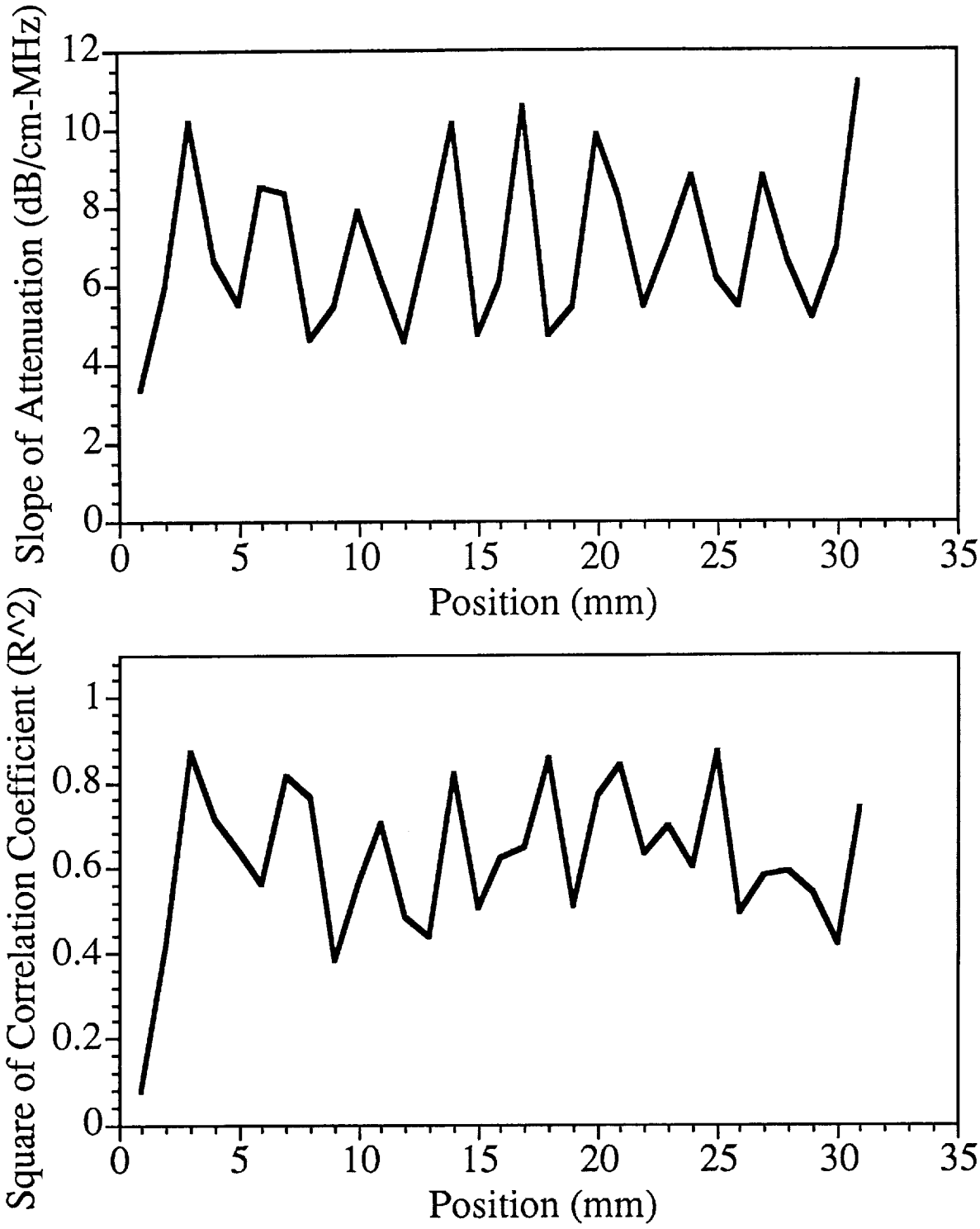

Figure 17 (a) Phase-sensitive slope-of-attenuation values over the upper row (as shown by the arrows in Figure 15b) in Region 3. (b) R^2 values for linear fit of phase-sensitive signal loss at each site in Figure 17a.

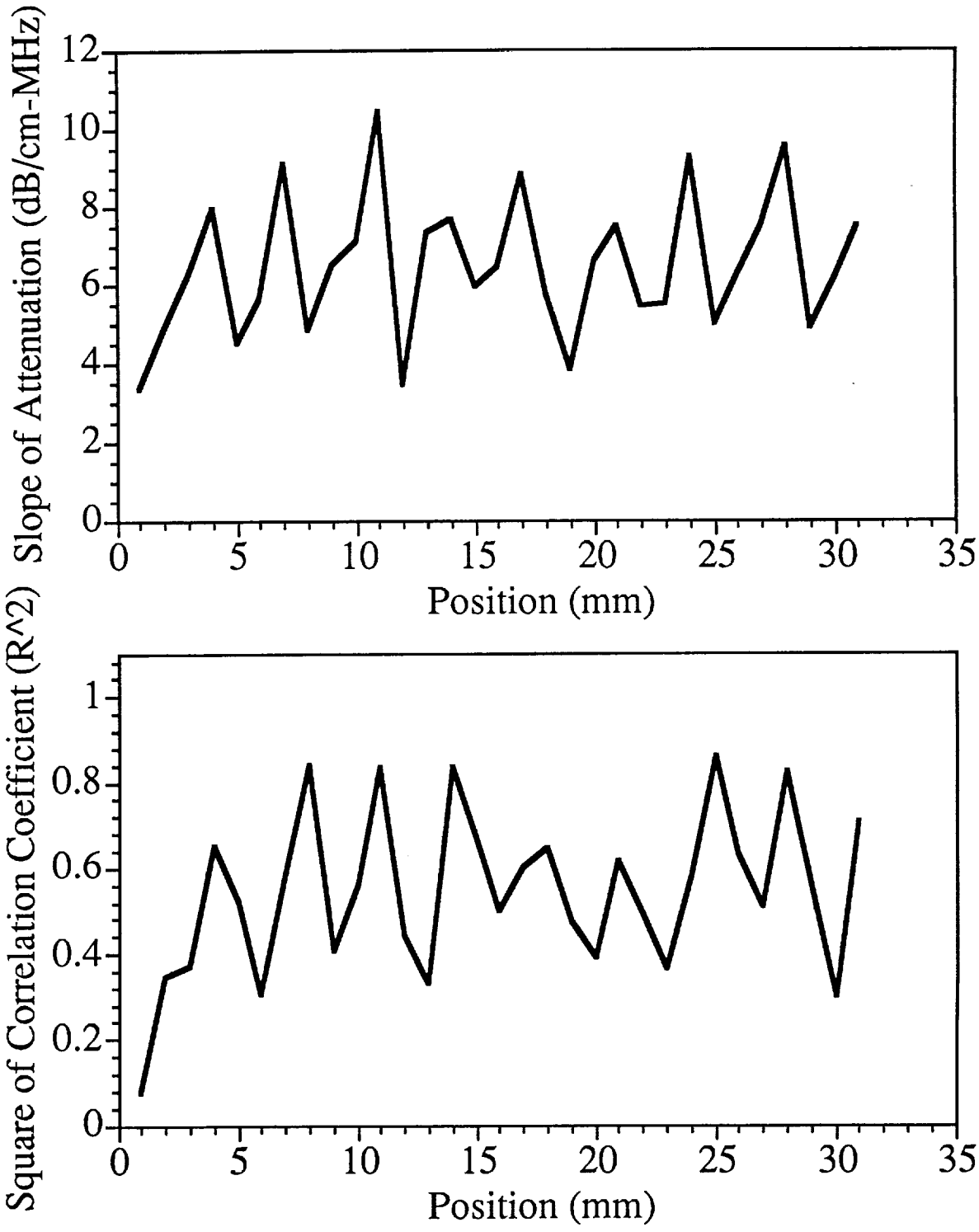

Figure 18 (a) Phase-sensitive slope-of-attenuation values over the lower row (as shown by the arrows in Figure 15b) in Region 3. (b) R^2 values for linear fit of phase-sensitive signal loss at each site in Figure 18a.

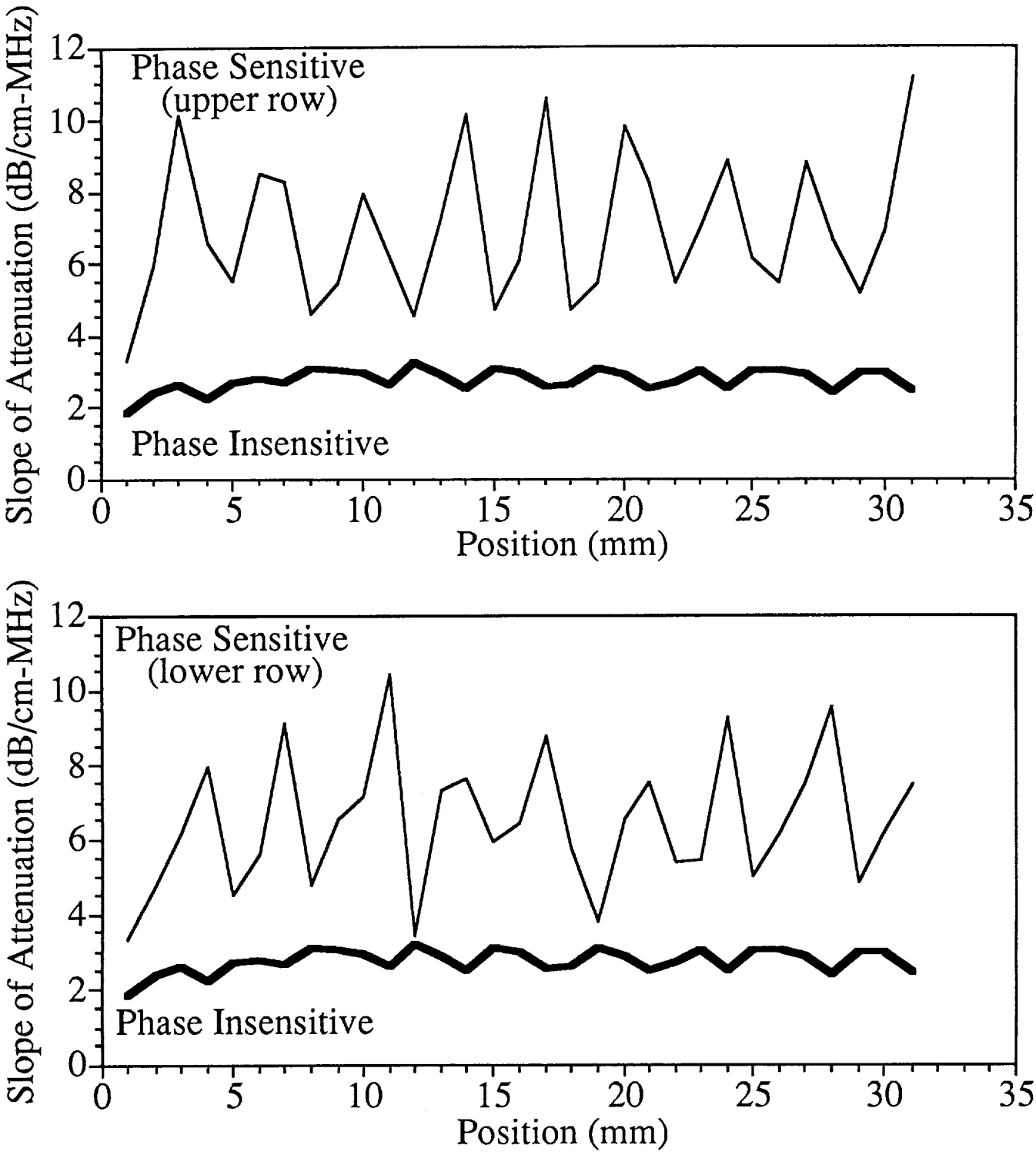

Figure 19 (a) Comparison of the phase-insensitive, acoustoelectric and the phase-sensitive slope-of-attenuation values in Region 3. The phase-sensitive values are from the upper line in Figure 15b. (b) Comparison of the phase-insensitive, acoustoelectric and the phase-sensitive slope-of-attenuation values in Region 3. The phase-sensitive values are from the lower line in Figure 15b.

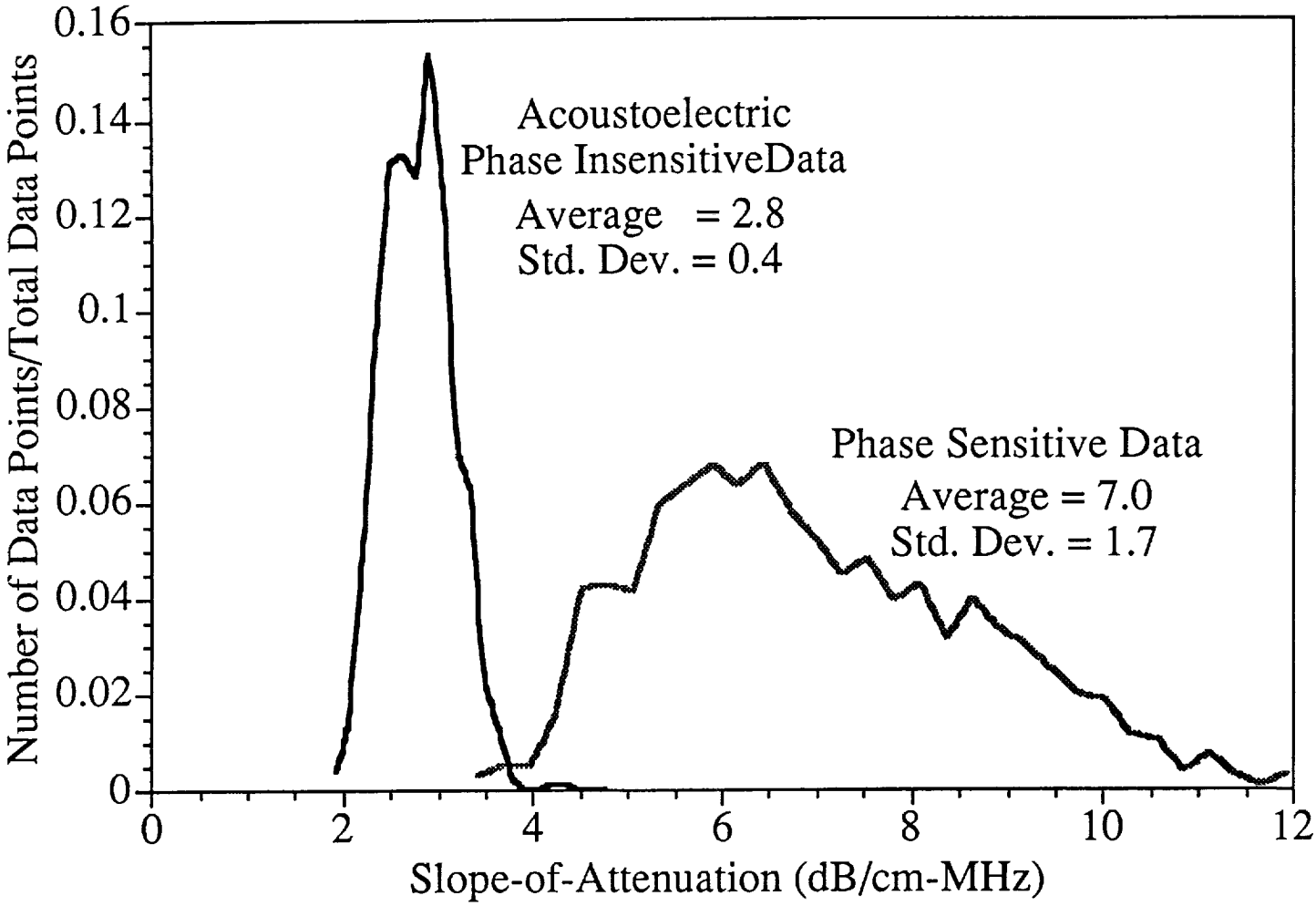

Figure 20. Plot of the normalized distribution of slope-of-attenuation values over all of Region 3 for both the acoustoelectric and phase-sensitive data.

V. Discussion

The results presented in this Progress Report indicate that phase-sensitive and phase-insensitive slope-of-attenuation measurements can yield markedly different results when used to characterize various regions and aspects of a complex structured carbon/epoxy panel. These results may aid in determining which ultrasonic methods/instruments are most appropriate for ascertaining the state of materials with complex structure and/or composition.

Previous investigations have suggested that phase-insensitive measurement systems can produce attenuation related data that is more characteristic of the bulk properties of a material.[1-3, 6]. Results of this investigation suggest that phase-insensitive interrogation of composites with stitching may also produce more reliable results because the measurements are more immune to the phase-cancellation effects due to ultrasonic velocity differences present in the interrogation of a stitched region. Furthermore, the acoustoelectric signal loss values may more

accurately reflect true ultrasonic losses in the material because they are not as susceptible to artifacts arising from phase-front distortion in the field. The effects of phase-front distortion manifest themselves as an underestimate of the energy contained in an incident ultrasonic field impinging on receiving transducers which are sensitive to the phase of the pressure field. This underestimation, due to phase-cancellation across the face of the transducer, is inherent in the receiving aperture and does not accurately reflect ultrasonic losses in the bulk material being characterized. Although the phase cancellation due to this distortion may enhance features of inhomogeneous materials, it can potentially mask the signal loss due to the bulk state of the medium. In inhomogeneous materials such as stitched composites phase-cancellation effects arising from propagation through the complex architecture may mask the presence of inherent flaws or defects. Phase-cancellation effects may contribute in many different ways to the measured frequency dependence of the signal loss. The slope-of-attenuation measurements made on the ballistically damaged carbon/epoxy specimen with phase-sensitive and phase-insensitive methods illustrate these effects.

Because the relatively large R^2 values associated with the fit of the acoustoelectric signal loss data at each sample point on the specimen attest to the linear nature of the dependence of the signal loss on frequency, the slope-of-attenuation appears to be a good parameter for characterization of the acoustoelectrically investigated regions of the specimen. However, the R^2 values associated with the phase-sensitive measurements may or may not be a good indication of the validity of the slope-of-attenuation values at each position on the specimen because the signature of the phase-cancellation effects in the measured bandwidth may vary for the different characteristic structures present in the specimen. Therefore it is possible that phase sensitive slope values whose linear fit yielded a high R^2 value were still corrupted by phase-cancellation effects.

The phase-sensitive values for the slope-of-attenuation along the stitching in Region 1 illustrate the distinct signatures of the phase-cancellation effects. The slope values for points which correspond to areas on the sample where the stitching runs across the specimen surface are significantly higher in magnitude than the corresponding acoustoelectrically obtained values, yet these phase-sensitive values have relatively good R^2 coefficients associated with their linear fits. When the phase-sensitive values for slope near the through-stitched areas are examined, some are found which are lower in value than the corresponding acoustoelectric values, but these sites also have very low R^2 values for the phase-sensitive data. Because the acoustoelectric data suggests that the signal loss is linear with frequency, the very low R^2 values for some of the phase-sensitive measurements can be interpreted as an artifact of phase-cancellation. We hypothesize that phase-cancellation effects, due to the different types of structures along the stitched line, may cause the phase-sensitive slope values to have a much wider variation than the

acoustoelectric slope values (see Figure 8) and may contribute to the shape of signal loss curves in different ways. The average value of the slope-of-attenuation for the phase-sensitive data along the stitch line is 10.8 dB/(cm-MHz) and these values collectively have a standard deviation of 4.8 dB/(cm-MHz). In contrast, the phase-insensitive average was 5.7 dB/(cm-MHz) with a standard deviation of 1.3 dB/(cm-MHz).

Similar results are seen when examining the data from Region 2. This region encompasses part of the damaged portion of the specimen and thus allows further comparisons beyond those carried out on Region 1. The portion of the stitch line in this region runs through both damaged and apparently undamaged sections of the specimen. When looking at the slope-of-attenuation values along this stitch line, the damaged and undamaged portions may be identified by different average slope values. This suggests that detecting a shift in the average slope-of-attenuation values over a region of interest large compared to the characteristic size of the inhomogeneous structures built in to a material may allow for the evaluation of damage in stitched composite materials. Although both the phase-sensitive and phase-insensitive data exhibited a shift in the average slope values between the two regions of the same order, the standard deviation of the phase-sensitive slope values along the entire line was an order of magnitude larger than that for the phase-insensitive data. The shift in the average values between the two segments was 4.4% of the standard deviation in the phase-sensitive case, while for the acoustoelectric data the level shift was 93.5% of the standard deviation. Thus phase-insensitive techniques may provide a more reliable method to identify damaged areas of stitched structures, since the variation in the phase-sensitively obtained values can serve to mask the average changes in material characteristics.

The phase-sensitive slope values for sampled sites in Region 3 (woven only region) displayed a much wider distribution than the corresponding phase-insensitive values over the same area (see Figure 20). This suggests that acoustoelectric methods of characterization may be more useful for woven materials due to their ability to obtain a more well-defined slope-of-attenuation value for this relatively structure-free region than the phase-sensitive methods.

Understanding the underlying physics in the interaction of ultrasound with 3-dimensional composite structures will be an important step in developing intelligent strategies for evaluating the mechanical integrity of advanced engineering materials. Our Laboratory continues to focus on the problems inherent in the quantification of mechanical properties of complex materials by utilizing a wide range of ultrasonic investigative techniques and methods of analysis to examine samples with intricate structural and geometric characteristics.

VI. References

1. L.J. Busse, J.G. Miller, D.E. Yuhas, J.W. Mimbs, A.N. Weiss, and B.E. Sobel, "Phase Cancellation Effects: A Source of Attenuation Artifact Eliminated by a CdS Acoustoelectric Receiver", *Ultrasound in Medicine*, Vol. 3, pp. 1519-1535, (1977).

2. J. S. Heyman and John H. Cantrell, "Application of an Ultrasonic Phase Insensitive Receiver to Material Measurements"((Published 1977), pp. 124-128.

3. J.S. Heyman, "Phase Insensitive Acoustoelectric Transducers", *J. Acoust. Soc. Am.*, Vol. **64**, pp. 243-249, (1978).

4. Mark R. Holland and J.G. Miller, "Phase-Insensitive and Phase-Sensitive Quantitative Imaging of Scattered Ultrasound Using a Two-Dimensional Pseudo-Array", *Proc. IEEE Ultrasonics Symposium*, (1988, Chicago), (Published 1989), Vol. 88 CH 2578-3, pp. 815-819.

5. Patrick H. Johnston and J.G. Miller, "A Comparison of Backscatter Measured by Phase Sensitive and Phase Insensitive Detection", *IEEE Trans. Ultrasonics, Ferroelectrics, and Frequency Control*, Vol. **UFFC-33**, pp. 78, (1986).

6. Patrick H. Johnston and A. A. Ananda, "The Role of Phase Cancellation in the Ultrasonic NDE of Stitched Graphite-Epoxy Composites", *IEEE Ultrasonics Symposium*, (1991, Orlando, FL), (Proc. IEEE Ultrasonics Symposium, 1991, Published 1992 (To be published)).

7. J.R. Klepper, G.H. Brandenburger, L.J. Busse, and J.G. Miller, "Phase Cancellation, Reflection, and Refraction Effects in Quantitative Ultrasonic Attenuation Tomography", *Proc. IEEE Ultrasonics Symposium, Phoenix*, Vol. **77 CH 1264-1SU**, pp. 182-188, (1977).

8. J.R. Klepper, G.H. Brandenburger, J.W. Mimbs, B.E. Sobel, and J.G. Miller, "Application of Phase Insensitive Detection and Frequency Dependent Measurements to Computed Ultrasonic Attenuation Tomography", *IEEE Trans. on Biomedical Engineering*, Vol. **BME-28**, pp. 186-201, (1981).

9. Peter W. Marcus and Edwin L. Carstensen, "Problems with Absorbtion Measurements of Inhomogeneous Solids", *J. Acoust. Soc. Am.*, Vol. **58**, pp. 1334-1335, (1975).

10. J.G. Miller, J. S. Heyman, D.E. Yuhas, and A. N. Weiss, "A Power Sensitive Transducer for Echocardiography and Other Medical Ultrasonic Applications", *Ultrasound in Medicine*, Vol. **1**, pp. 447-453, (1975).

11. Kelly M. Pan and C.N. Liu, "Tomographic Reconstruction of Ultrasonic Attenuation with Correction for Refractive Errors", *IBM J. Res. Develop.*, Vol. **25**, pp. 71-82, (1981).